Follow us @BoneJointRes

Freely available online OPEN ACCESS

BJR

INFECTION

Application of ^{68}Ga-citrate PET/CT for differentiating periprosthetic joint infection from aseptic loosening after joint replacement surgery

T. Xu,
Y. Zeng,
X. Yang,
G. Liu,
T. Lv,
H. Yang,
F. Jiang,
Y. Chen

From The Affiliated Hospital of Southwest Medical University, Luzhou, China

Aims

We aimed to evaluate the utility of ^{68}Ga-citrate positron emission tomography (PET)/CT in the differentiation of periprosthetic joint infection (PJI) and aseptic loosening (AL), and compare it with ^{99m}Tc-methylene bisphosphonates (^{99m}Tc-MDP) bone scan.

Methods

We studied 39 patients with suspected PJI or AL. These patients underwent ^{68}Ga-citrate PET/CT, ^{99m}Tc-MDP three-phase bone scan and single-photon emission CT (SPECT)/CT. PET/CT was performed at ten minutes and 60 minutes after injection, respectively. Images were evaluated by three nuclear medicine doctors based on: 1) visual analysis of the three methods based on tracer uptake model, and PET images attenuation-corrected with CT and those not attenuation-corrected with CT were analyzed, respectively; and 2) semi-quantitative analysis of PET/CT: maximum standardized uptake value (SUVmax) of lesions, SUVmax of the lesion/SUVmean of the normal bone, and SUVmax of the lesion/SUVmean of the normal muscle. The final diagnosis was based on the clinical and intraoperative findings, and histopathological and microbiological examinations.

Results

Overall, 23 and 16 patients were diagnosed with PJI and AL, respectively. The sensitivity and specificity of three-phase bone scan and SPECT/CT were 100% and 62.5%, 82.6%, and 100%, respectively. Attenuation correction (AC) at 60 minutes and non-AC at 60 minutes of PET/CT had the same highest sensitivity and specificity (91.3% and 100%), and AC at 60 minutes combined with SPECT/CT could improve the diagnostic efficiency (sensitivity = 95.7%). Diagnostic efficacy of the SUVmax was low (area under the curve (AUC) of ten minutes and 60 minutes was 0.814 and 0.806, respectively), and SUVmax of the lesion/SUVmean of the normal bone at 60 minutes was the best semi-quantitative parameter (AUC = 0.969).

Conclusion

^{68}Ga-citrate showed the potential to differentiate PJI from AL, and visual analysis based on uptake pattern of tracer was reliable. The visual analysis method of AC at 60 minutes, combined with ^{99m}Tc-MDP SPECT/CT, could improve the sensitivity from 91.3% to 95.7%. In addition, a major limitation of our study was that it had a limited sample size, and more detailed studies with a larger sample size are warranted.

Cite this article: *Bone Joint Res* 2022;11(6):398–408.

Keywords: ^{68}Ga-citrate, PET/CT, ^{99m}Tc-MDP, Periprosthetic joint infection, Aseptic loosening

Correspondence should be sent to Yue Chen; email: chenyue5523@126.com

doi: 10.1302/2046-3758.116.BJR-2021-0464.R1

Bone Joint Res 2022;11(6):398–408.

Article focus

- Exploring the effectiveness of ^{68}Ga-citrate as an auxiliary diagnostic tool for periprosthetic joint infection (PJI) and aseptic loosening (AL) following joint arthroplasty surgery.

Key messages

- Visual analysis methods of attenuation correction (AC) at 60 minutes and non-AC at 60 minutes, and semi-quantitative analysis parameter of maximum standardized uptake value (SUVmax) of the

lesion/SUVmean of the normal bone at 60 minutes are effective for the differential diagnosis of PJI and AL.
- ^{68}Ga-citrate positron emission tomography (PET)/CT has a certain false negative rate for the diagnosis of PJI, and thus needs to be combined with bone imaging.
- Combining ^{68}Ga-citrate PET/CT with ^{99m}Tc-MDP single-photon emission CT (SPECT)/CT can improve the diagnostic efficiency.

Strengths and limitations

- This is the first study differentiating diagnosis of PJI and AL using ^{68}Ga-citrate PET/CT.
- This study involved a single centre, with a relatively small sample size.
- Image analysis standards of ^{68}Ga-citrate were formulated mainly based on experience from relevant studies of ^{18}F-FDG and ^{18}F-F-sodium fluoride (NaF), which is a potential flaw.

Introduction

The causes of pain following joint arthroplasty include aseptic loosening (AL), periprosthetic joint infection (PJI), periprosthetic fracture, and heterotopic ossification.[1] Of these, AL and PJI are the commonest complications,[2] and accurately distinguishing between the two is essential because treatment approaches for the two conditions differ substantially. In the presence of AL, a one-stage revision arthroplasty is typically successful, whereas PJI is more devastating, and the treatment is more complex.[3-6] The available treatment options for PJI include antibiotic therapy without operation, debridement with implant retention, and single-stage or two-stage revision arthroplasty,[3] and the specific treatment choice mainly depends on the patient's condition. An accurate and timely diagnosis can ensure that the correct treatment strategy is selected. However, the differentiation of AL from low-virulence PJI remains a challenge due to the similarities in their associated symptoms.[7] Further, most infections that are identified are chronic and low-grade, lacking the typical clinical symptoms and signs associated with an infection.[4,7]

Various methods are currently used in the preoperative diagnosis of AL and PJI, including laboratory testing, X-ray scans, CT, ^{99m}Tc-methylene bisphosphonates (^{99m}Tc-MDP) bone scan, ^{67}Ga-citrate imaging, radioactive-labelled leucocyte scintigraphy, joint aspiration, and microbial culture.[3,4,8] However, there is no unified diagnostic protocol for the evaluation of AL and PJI, and each of these methods has shortcomings.[9] Although most studies indicate that combined ^{111}In-labelled leucocyte/^{99m}Tc-sulphur colloid marrow imaging is accurate, it is hampered by time-intensive labelling process, poor spatial resolution, and limited availability.[8,9] At present, different scoring systems are available for diagnosing PJI. Alt et al[10] creatively put forward the concept of the PJI-TNM (T–tissue and implant conditions, N–non-human cells (bacteria and/or fungi), M–morbidity of the patient) system. However, the preoperative diagnostic process may provide insufficient information for a definite diagnosis prior to surgery, and this can affect treatment decisions; this highlights the importance of an accurate preoperative diagnosis for planning effective treatment strategies.

Ga-68 is an isotope of Ga-67 with similar physical and chemical properties,[11] and it is obtained by a Ge-68/Ga-68 generator which can be used on demand. In addition, as a positron radiopharmaceutical, ^{68}Ga-citrate has a suitable half-life (68 minutes) for high-resolution imaging. The preliminary data on the ability of ^{68}Ga-citrate positron emission tomography (PET) imaging to identify bone infections are promising.[12,13] Salomäki et al[13] demonstrated that ^{68}Ga-citrate was able to distinguish between bone infections and physiological bone healing following surgery to the bone. Data from Tseng et al[12] suggested that ^{68}Ga-citrate PET/CT may distinguish infectious from non-infectious diseases after joint arthroplasty. However, research on the efficacy of ^{68}Ga-citrate PET/CT in distinguishing between PJI and AL is limited. We hypothesized that ^{68}Ga-citrate can distinguish between PJI and AL, especially in the early postoperative period, and explored the effectiveness of ^{68}Ga-citrate as an auxiliary diagnostic tool for PJI and AL following joint arthroplasty surgery.

Methods

Patients. This was a prospective study. In our hospital, a total of 47 patients who were suspected of having PJI or AL were recruited, based on our inclusion/exclusion criteria, between August 2019 and May 2021. These patients underwent ^{68}Ga-citrate PET/CT imaging; in addition, all patients underwent ^{99m}Tc-MDP three-phase bone scan and single-photon emission computed tomography (SPECT)/CT within one week prior to ^{68}Ga-citrate PET/CT imaging. All patients underwent anteroposterior (AP) and lateral X-ray of hip joint or knee joint and laboratory examination, such as evaluation of serum inflammatory markers, before SPECT/CT and PET/CT imaging. Most of the joint aspirate was arranged before SPECT/CT and PET/CT imaging. Variables including age, sex, involved joint, cause of implant, time after implant, main symptoms, and laboratory examination were recorded. All procedures of this study were carried out in accordance with the principles of the Helsinki Declaration.[14] This study was approved by the ethics committee of our hospital (AHSWMU-2019-07). All patients provided written informed consent after the nature and significance of the imaging study had been fully explained to them.

Inclusion and exclusion criteria. The inclusion criteria of the study were as follows: 1) a history of hip or knee arthroplasty, and the postoperative time is more than three months (based on the possibility of abnormal bone dynamic imaging within three months after surgery);[15] 2) the main clinical manifestation of the patient is prosthetic joint pain that was suspected to be PJI or AL; and 3) the patient is planned for surgery (if at least two cultures that yield the same organism or at least one virulent microorganism in the preoperative synovial fluid culture,

Table I. Visual analysis standards for different imaging methods.

Disease	Three-phase bone scan[15]	SPECT/CT[17]	^{68}Ga-citrate PET/CT[12,18]
Periprosthetic joint infection	Positive perfusion and/or blood pool and positive delayed phase.	Hip joint: diffuse tracer uptake in the acetabulum and/or femoral prosthesis. Knee joint: diffuse tracer uptake in the tibial or femoral component.	Diffuse tracer uptake in the bone-prosthesis interface and/or abnormal tracer uptake in the periprosthetic soft-tissue. (Mild tracer uptake limited to soft-tissues and/or synovium adjacent to the neck of the hip prosthesis or synovium of knee joint prosthesis was not considered sufficient to classify as infection.)
Aseptic loosening	Negative perfusion and blood pool but positive delayed phase.	Hip joint: focal tracer uptake at the acetabulum and/or trochanter region and/or femoral prosthetic tip. Knee joint: focal tracer uptake at the tibial tray and keel and/or posterior region of femoral condyles.	No abnormal tracer uptake or just small focal tracer uptake in the stress point of the prosthesis, and without abnormal uptake of periprosthetic soft-tissue.

PET, positron emission tomography; SPECT, single-photon emission CT.

Table II. Diagnostic criteria for periprosthetic joint infection and aseptic loosening (according to 2013 Infectious Disease Society of America).[21]

Periprosthetic joint infection (≥ 1 positive criteria)	Aseptic loosening
1. Sinus tract that communicates with the prosthesis or the presence of purulence without another known aetiology surrounding the prosthesis.	Three positive criteria were all negative, and surgery confirmed the loosening of at least one prosthetic part.
2. Acute inflammation as seen on histopathologic examination of periprosthetic tissue.	
3. At least two cultures that yield the same organism. The growth of a virulent microorganism (e.g. *Staphylococcus aureus*) in a single specimen is also considered as indicative of a periprosthetic joint infection.	

or if there is a sinus tract communicating with the prosthesis, the surgery is not compulsory). All patients were followed up for at least three months. The exclusion criteria of the study were as follows:[16] 1) less than 18 years old, pregnancy, or lactation; 2) the presence of another inflammatory arthropathy or osteopathy in the affected joint; 3) treatment with antibiotics before the study; 4) infection or inflammation of other body parts; and 5) critical illness or unstable vital signs.

Drop-out criteria. The drop-out criteria were as follows: 1) patients who did not undergo surgery and could not also be definitely diagnosed by clinical manifestation and preoperative puncture; and 2) through clinical manifestations, intraoperative findings, microbial culture, and histopathological examination, neither PJI nor AL was considered, and as a result other diagnoses were considered.

^{99m}Tc-MDP bone scan. After an intravenous injection of ^{99m}Tc-MDP ranging from 740 to 925 MBq, dynamic flow images of the area of interest were obtained for 60 seconds (two seconds/frame), immediately followed by blood pool, and delayed static images at one to five minutes and three to four hours after injection, respectively.

Synthesis of ^{68}Ga-citrate and PET/CT scanning. An Isotopen Technologies Garching (ITG) Ge-68/Ga-68 generator (China Isotope and Radiation Corporation, China) was washed with 0.05 M HCl, and 5 ml Gallium-68^{3+} solution was obtained for radioactive labelling. In the process of washing, the Gallium-68^{3+} solution was divided into five tubes, each containing 1 ml of the solution. The second to fourth tubes of Gallium-68^{3+} (20 mCi) containing 3 ml in total were used. Sodium citrate solution (0.2 M) was prepared, and 1 ml sodium citrate was added to Gallium-68^{3+}. The mixture was allowed to react at room temperature for 15 minutes. Microorganisms were filtered through a 0.22 μm filter membrane. With 0.1 M ammonium acetate and methanol (1:1, v/v) as the developing solvent, the radiochemical purity of ^{68}Ga-citrate was analyzed by thin layer chromatography. The final radiochemical purity of the product was confirmed to be > 95%, with a pH ranging from 6 to 7. The injection dose of ^{68}Ga-citrate used was 3.7 MBq/kg. Local PET/CT scanning of the diseased joint was performed on a Philips Gemini TF 16 scanner (Philips Healthcare, The Netherlands) at ten minutes and 60 minutes after the injection of the intravenous tracer.

Image analysis. Three experienced nuclear medicine physicians (TX, HD, and XY) performed visual analysis (three-phase bone scan, SPECT/CT, and PET/CT) and semi-quantitative analysis (PET/CT). Interobserver differences in the interpretation of the images were resolved through discussion and reached a diagnostic consensus.

Visual analysis of three-phase bone scan, SPECT/CT, PET/CT images. The visual analysis criteria for different imaging methods are shown in Table I. We analyzed the PET/CT images collected at ten minutes and 60 minutes, respectively. To avoid CT over attenuation correction (AC) caused by metal implants and thus resulting in artifacts in PET images, both non-attenuation-corrected and attenuation-corrected PET images were visually assessed in all patients. In addition, mild or moderate uptake distributed uniformly and symmetrically along the edge of the prosthesis on SPECT/CT or ^{68}Ga-citrate PET/CT was non-specific uptake.

Semi-quantitative analysis. Semi-quantitative analysis of both ten minutes and 60 minutes PET/CT images was performed. A total of five volumes of interest were manually

Table III. Clinical features of the 39 patients.

Variable	Periprosthetic joint infection (n = 23)	Aseptic loosening (n = 16)	Total (n = 39)
Mean age, yrs (SD)	61.9 (12.3)	63.2 (9.2)	62.4 (11.0)
Sex, n (%)			
Female	7 (30.4)	8 (50)	15 (38.5)
Male	16 (69.6)	8 (50)	24 (61.5)
Clinical presentations, n (%)			
Fever	3 (13.0)	0 (0)	3 (7.7)
Joint pain	18 (78.3)	14 (87.5)	32 (82.1)
Joint swelling	9 (39.1)	4 (25)	13 (33.3)
Local pyrexia	10 (43.5)	0 (0)	10 (25.6)
Exudate	9 (39.1)	0 (0)	9 (23.1)
Mean number of laboratory examinations (SD)			
White blood cell (10^9/l)	8.6 (5.7)	7.6 (2.7)	8.3 (4.9)
Neutrophil granulocyte (10^9/l)	6.3 (5.2)	5.2 (2.2)	5.9 (4.5)
Neutrophil ratio (%)	68.0 (10.8)	67.6 (12.3)	67.8 (11.1)
ESR (mm/h)	52.7 (41.9)	18.8 (8.1)	41.8 (38.1)
CRP, ng/ml	31.8 (56.9)	2.77 (1.5)	24.0 (50.1)
Prosthesis location, n (%)			
Hip	11 (47.8)	10 (62.5)	21 (53.8)
Knee	12 (52.2)	6 (37.5)	18 (46.2)
Cause of joint arthroplasty, n (%)			
Osteoarthritis	11 (47.8)	5 (31.3)	16 (41.0)
Avascular necrosis	4 (17.4)	4 (25.0)	8 (20.5)
Trauma	2 (8.7)	5 (31.3)	7 (17.9)
Fracture	3 (13.0)	1 (6.3)	4 (10.3)
Congenital dysplasia	1 (4.3)	0 (0)	1 (2.6)
Suppurative arthritis	1 (4.3)	0 (0)	1 (2.6)
Osteosarcoma	1 (4.3)	0 (0)	1 (2.6)
Giant cell tumour of bone	0 (0)	1 (6.3)	1 (2.6)
Mean prosthesis age, mths (SD)	42.4 (78.9)	54.5 (48.9)	47.3 (67.7)

SD, standard deviation.

drawn on PET/CT images. Volumes of interest covered the entire bone-prosthesis interface as well as periprosthetic soft-tissue (after the exclusion of vascular radioactivity). For reference organ uptake measurement, the mean standardized uptake value (SUVmean) of the nonaffected normal bone and muscle was measured. Normal bone uptake was measured by drawing volumes of interest over the nonaffected normal contralateral bones. Normal muscle uptake was measured using volumes of interest drawn over the contralateral thigh muscles. Using SUVmax of the lesion, SUVmax of the target area/SUVmean of the non-target area (SUVmax of the lesion/SUVmean of the normal bone and SUVmax of the lesion/SUVmean of the normal muscle) as semi-quantitative parameters,[19] the location of the lesions was determined by bone imaging when no obvious uptake abnormalities were identified on PET/CT imaging.

Final diagnostic criteria. The final diagnosis was based on clinical and intraoperative findings, and histopathological and microbiological examinations (five periprosthetic tissue/fluid samples).[20] The specific criteria are shown in Table II.

Statistical analysis. We preliminarily studied ten cases of PJI and AL in advance. The inclusion, exclusion, and dropout criteria for these ten patients were completely consistent with those adopted in this study. The sample size was estimated using the statistical software PASS (Version 15.0.5; NCSS, LLC, USA, 2017). Based on a sensitivity of 83.3% and specificity of 100% using PET/CT (using AC at 60 minutes as an evaluation method) and an expected prevalence of PJI of 60% in our sample (6/10), PASS 15.0 calculated that at least 48 patients should be recruited (23 cases of PJI, 15 cases of AL, and an additional ten cases as expected number of dropouts). However, recruitment was stopped at 47 cases because the number of PJI and AL cases met our expectations. Statistical software R (Version 4.1.1; R Core Team, R Foundation for Statistical Computing, Austria, 2021) was used for data analysis and description. The data are presented as mean and standard deviation (SD). For univariate diagnosis models, parameters including sensitivity, specificity, positive predictive value, and negative predictive value were used to evaluate the diagnostic value. In semi-quantitative analysis, we also performed receiver operating characteristic (ROC) analysis to obtain a cut-off value and area under the curve (AUC). For combined visual analysis models, logistic regression model was used to estimate the conditional probability of being in the four

Table IV. Single diagnostic value of six visual analysis indexes.

Index	TP	FP	TN	FN	Sen (%)	Spe (%)	NPV (%)	PPV (%)
Three-phase bone scan	23	6	10	0	100.0	62.5	100.0	79.3
SPECT/CT	19	0	16	4	82.6	100.0	80.0	100.0
Attenuation correction at 10 mins	20	0	16	3	87.0	100.0	84.2	100.0
Attenuation correction at 60 mins	21	0	16	2	91.3	100.0	88.9	100.0
Non-attenuation correction at 10 mins	21	0	16	3	87.0	100.0	84.2	100.0
Non-attenuation correction at 60 mins	21	0	16	2	91.3	100.0	88.9	100.0

FN, false negative; FP, false positive; NPV, negative predictive value; PPV, positive predictive value; Sen, sensitivity; Spe, specificity; SPECT, single-photon emission CT; TN, true negative; TP, true positive.

Table V. Combination of different visual analysis methods.

Combined model	Sen (%)	Spe (%)	NPV (%)	PPV (%)	Youden index
Attenuation correction at 60 min+ SPECT/CT	95.7	100.0	94.1	100.0	0.957
Attenuation correction at 60 min+ three-phase bone scan	91.3	100.0	88.9	100.0	0.913
SPECT/CT + three-phase bone scan	82.6	100.0	80.0	100.0	0.826
Attenuation correction at 60 min+ SPECT/CT + three-phase bone scan	95.7	100.0	94.1	100.0	0.957

NPV, negative predictive value; PPV, positive predictive value; Sen, sensitivity; Spe, specificity; SPECT, single-photon emission CT.

groups when given pre-defined variables; then, the conditional probability was used as a new index for the combined diagnosis. Statistical significance level was set at $p < 0.05$.

Results

Patient characteristics. Of the 47 recruited patients, eight cases dropped out of the study (five patients did not undergo surgery and/or microbiological culture for further definite diagnosis; one patient was pathologically confirmed as Langerhans cell histiocytosis; and two patients were not found to have infection or loosening during the surgery and were finally considered as metal-induced reactive tissue lesion). Finally, a total of 39 patients were included, which comprised 24 males and 15 females (mean age 62.4 years (SD 11 months)), with 21 cases of artificial hip joints and 18 cases of artificial knee joints. The mean time since surgery was 47.3 months (SD 67.7). A total of 23 cases of PJI and 16 cases of AL were diagnosed. Details of the patients are presented in Table III.

Visual analysis results. The evaluation of different visual analysis methods is shown in Table IV. Among all the visual analysis methods, ^{99m}Tc-MDP three-phase bone scan had the highest sensitivity (100%), but the specificity was lowest (62.5%). The sensitivity and specificity of ^{99m}Tc-MDP SPECT/CT were 82.5% and 100%, respectively. The sensitivity and specificity of AC at 60 minutes and non-AC at 60 minutes were high (91.3% and 100%, 91.3% and 100%, respectively).

The evaluation of combined visual analysis models is shown in Table V. The results showed that the combination of AC at 60 minutes and ^{99m}Tc-MDP SPECT/CT can maximize the diagnostic performance (sensitivity and specificity were 95.7% and 100%, respectively). The combined diagnostic efficacy of AC at 60 minutes, ^{99m}Tc-MDP SPECT/CT, and three-phase bone scan was the same as that of the former (sensitivity and specificity were 95.7% and 100%, respectively). However, the combination of ^{99m}Tc-MDP SPECT/CT and three-phase bone scan or three-phase bone scan and AC at 60 minutes cannot effectively improve the diagnostic efficiency.

Semi-quantitative analysis results. The ROC curves of the six semi-quantitative parameters are shown in Figure 1, and a comparison of six semi-quantitative parameters between PJI and AL is shown in Table VI. SUVmax of the lesion/SUVmean of the normal bone at 60 minutes was the best semi-quantitative parameter in this study (AUC = 0.969), with a sensitivity and specificity of 91.3% and 93.8%, respectively. The diagnostic efficacy of SUVmax of the lesion/SUVmean of the normal muscle at 60 minutes was the second highest (AUC was 0.909), with a sensitivity and specificity of 69.6% and 100%, respectively. Among all the semi-quantitative parameters, SUVmax had the worst differential diagnosis ability (AUC of SUVmax of lesions at ten minutes and SUVmax of lesions at 60 minutes was 0.814 and 0.806, respectively).

Discussion

Accurately distinguishing PJI from AL preoperatively is essential for optimal treatment. Currently, the diagnostic criteria ruling implant-associated infection have become ever more accurate and there are different typing systems that can be used in the differential diagnosis of PJI and AL. However, the detection of the causative pathogen still relies mostly on conventional microbial culture, and the main demerit of preoperative puncture bacterial culture is that it is time-consuming, and the positive rate of culture is low.[22,23] Several methods can be used in the preoperative diagnosis of PJI and AL, including laboratory tests for inflammatory biomarkers,[24,25] synovial fluid marker

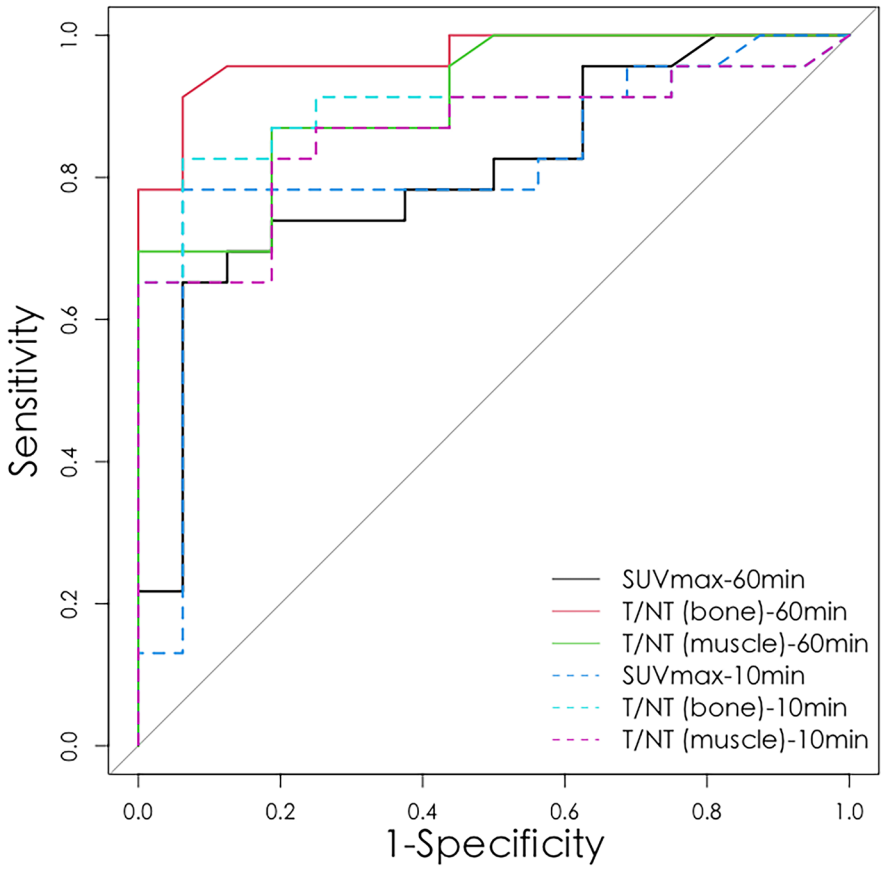

Fig. 1

The receiver operating characteristic curves of maximum standardized uptake value (SUVmax) of lesions, SUVmax of the lesion/SUVmean of the normal bone, and SUVmax of the lesion/SUVmean of the normal muscle. T/NT, SUVmax of target region/SUVmean of non-target region.

Table VI. Single diagnostic value of six semi-quantitative analysis indexes.

Index	Cut-off*	AUC	Sen (%)	Spe (%)	NPV (%)	PPV (%)
SUVmax of the lesion at 10 mins	2.6	0.814	78.3	93.8	75.0	94.7
SUVmax of the lesion at 60 mins	2.9	0.806	65.2	93.8	65.2	93.8
SUVmax of the lesion/SUVmean of the normal bone at 10 mins	3.5	0.895	82.6	93.8	78.9	95.0
SUVmax of the lesion/SUVmean of the normal bone at 60 mins	3.4	0.969	91.3	93.8	88.2	95.5
SUVmax of the lesion/SUVmean of the normal muscle at 10 mins	5.7	0.863	65.2	100.0	66.7	100.0
SUVmax of the lesion/SUVmean of the normal muscle at 60 mins	6.0	0.909	69.6	100.0	69.6	100.0

*When it is greater than or equal to the cut-off value, it is predicted to be diagnosed as a group of periprosthetic joint infections.
AUC, area under the curve; NPV, negative predictive value; PPV, positive predictive value; Sen, sensitivity; Spe, specificity; SUV, standardized uptake value.

tests,[23–31] and imaging examination.[4,12,18,19,32–39] Recently, promising results have been reported regarding synovial biomarker tests, including the neutrophil CD64 index, synovial interleukin (IL)-6 measurement, metagenomic next-generation sequencing, enzyme-linked immunosorbent assay (ELISA) methods to detect the concentration of calprotectin, RNA-based transcription-quantitative polymerase chain reaction method, and lateral flow test.[23–31] Although these studies show that the above indices or methods perform well in identifying infected and non-infectious lesions, there were some limitations, including lack of practical experience in large samples, unavailability of the assays in some laboratories, and conflicts between different studies, which make the test results difficult to interpret. At present, preoperative non-invasive imaging examination is an attractive method, wherein nuclear medical examination, which can reflect functional changes, has unique advantages.

Preliminary data on the use of ^{68}Ga-citrate PET/CT to identify bone infections are promising.[12,13] Importantly, these studies have shown that ^{68}Ga-citrate PET/CT may differentiate between bone infection and physiological

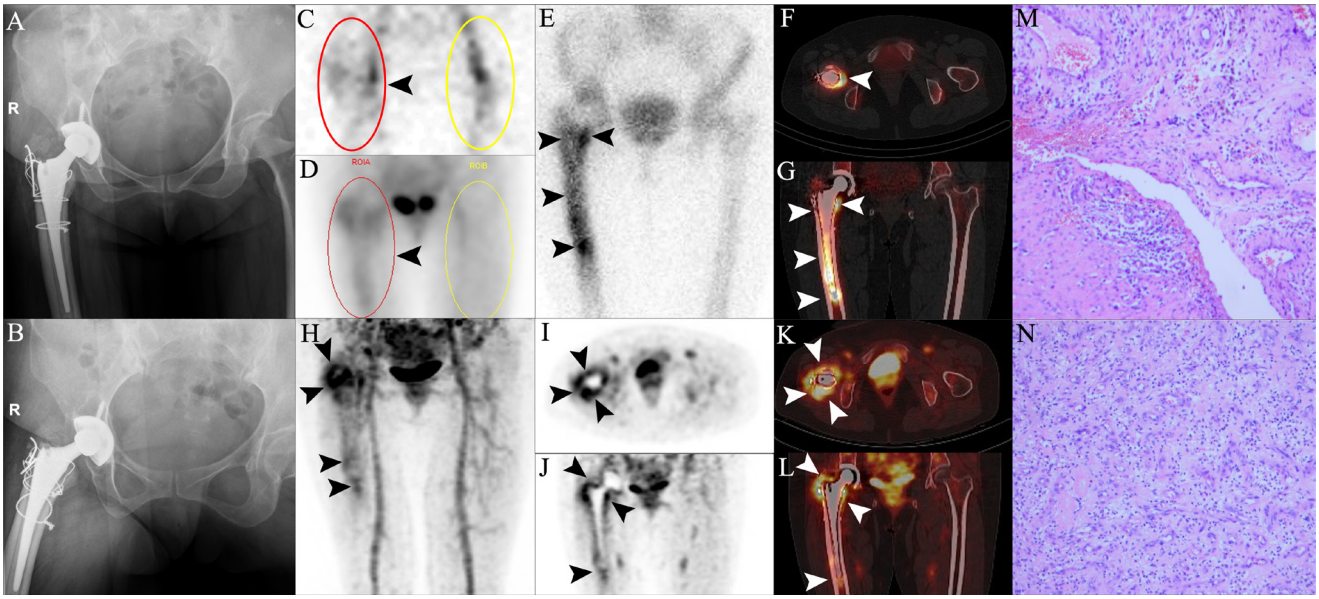

Fig. 2

Positive findings for infection in the three-phase bone scan, single-photon emission CT (SPECT)/CT, and positron emission tomography (PET)/CT in a patient with periprosthetic joint infection (PJI) confirmed by microbiological culture of *Staphylococcus aureus* and *Escherichia coli*. A 46-year-old woman underwent right hip arthroplasty for traumatic osteoarthritis in 2018, and developed pain in the right hip joint in April 2020. a) and b) Anteroposterior (AP) and lateral radiographs of the right hip joint at two years postoperatively showed an uneven decrease in bone density around the prosthesis. c) to e) ^{99m}Tc-MDP three-phase bone scan showed positive perfusion, blood pool, and delayed phase in the right hip (arrowheads) (red circles of c) to d) – region of interest of the affected side; yellow circles of c) to d) – region of interest of the normal side). f) and g) SPECT/CT revealed a diffuse increase in bone metabolism in the femoral prosthesis (arrowheads). h) to l) ^{68}Ga-citrate PET/CT showed uneven diffuse uptake of the right femur trochanter around the soft-tissue and the distal femoral prosthesis (arrowheads). The patient underwent surgical treatment, and a large amount of pus was found in the right hip joint. m) and n) Histopathological examination revealed many neutrophils, lymphocytes, and plasma cells (haematoxylin and eosin (H&E) 200×). Microbial culture showed the presence of *Staphylococcus aureus* and *Escherichia coli*. PJI of the right hip was diagnosed.

bone healing after bone surgery,[13] and distinguish infectious from non-infectious diseases after joint arthroplasty.[12] Our preliminary results revealed that visual analysis methods of AC at 60 minutes and non-AC at 60 minutes could be used to distinguish AL from PJI with high sensitivity and specificity (91.3% and 100%, 91.3% and 100%, respectively), and they had a very high positive predictive value for the diagnosis of PJI (Figures 2 and 3). We also reviewed previous studies regarding the diagnosis of PJI and AL using PET or PET/CT. Tseng et al[12] found that the sensitivity and specificity of ^{68}Ga-citrate PET/CT in diagnosing PJI were 92% and 88%, respectively. This is different from our findings and may be related to the use of different visual analysis standards in the two studies. Kim and Kim[32] analyzed 25 studies that evaluated PJI and found a sensitivity of 88% for PET or PET/CT (^{18}F-FDG, ^{18}F-sodium fluoride (^{18}F-NaF), or ^{18}F-FDG-leukocyte) and a specificity of 89%. Further, ^{18}F-FDG-leukocyte PET/CT has been reported to have a high efficiency in distinguishing PJI and AL (the sensitivity and specificity being 93.3% and 97.4%, respectively).[33] Several studies on the use of ^{18}F-FDG PET in the differential diagnosis of PJI and AL have shown different results, with a sensitivity and specificity of 14% to 94.87%, and 38.56% to 95%, respectively.[34–38] In addition, ^{18}F-NaF showed a good prospect in the differential diagnosis of PJI and AL, with a sensitivity and specificity of 75% to 95%, and 88% to 100%, respectively;[4,18,19,39] its best diagnostic efficacy in a study (sensitivity and specificity being 92.9% and 100%, respectively)[19] was slightly higher than that observed in this study.

In addition, ^{68}Ga-citrate is not a specific infection imaging agent, and tracer uptake can also be found in aseptic inflammation, as shown in osteoarthritis (OA) (Figure 3). However, the uptake pattern of the OA case and all cases of AL in our study was mainly mild focal uptake; some cases also showed no uptake, and the cases of PJI mainly showed diffuse uptake. In previous studies, possible mechanisms of ^{68}Ga-citrate accumulation in PJI were interpreted as: binding to transferrin; binding to ferritin in bacteria and lactoferrin in neutrophils; direct absorption by siderophores with a high affinity for Ga-68; and enhanced capillary permeability at the lesion site.[12,40,41] AL is described as a loss of fixation of the implant that can occur because of inadequate initial fixation and mechanical loss of fixation over time.[42,43] In addition, particles of wear debris may lead to macrophage activation, which in turn releases bone-resorbing products.[43,44] This results in bone osteolysis around the implant, resulting in the biological loss of fixation.[35,43] Therefore, AL may be accompanied by an inflammatory immune reaction to the prosthetic material, which makes it possible for the imaging of patients with AL to show the uptake of ^{68}Ga-citrate to a certain extent. However, the

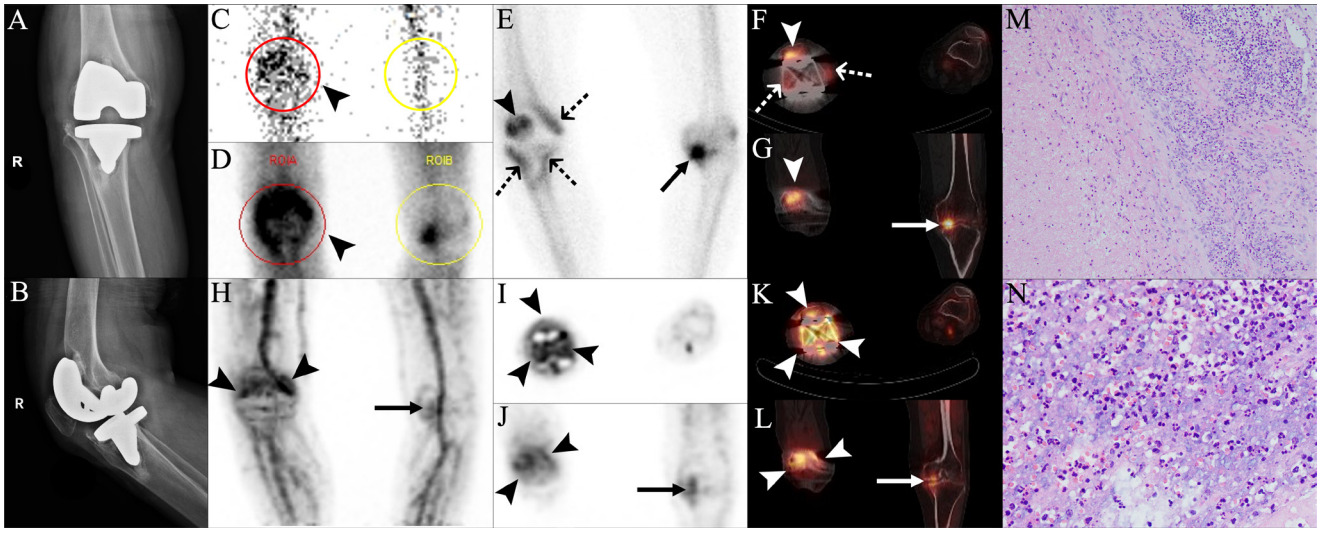

Fig. 3

True positive findings in three-phase bone scan and positron emission tomography (PET)/CT, and false negative findings for infection in single-photon emission CT (SPECT)/CT, in a patient with periprosthetic joint infection (PJI) caused by *Staphylococcus epidermidis*. A 66-year-old man underwent right knee arthroplasty for osteoarthritis (OA) in December 2019, and he developed pain and exudate in the right knee in March 2020. Further, physical examination showed swelling of the right knee joint, with a sinus tract that communicated with the prosthesis. a) and b) Anteroposterior (AP) and lateral radiographs of the right knee joint at three months postoperatively showed obvious swelling of the right knee joint and an uneven decrease in bone density around the prosthesis. The patient was diagnosed with PJI, considering the above symptoms. The patient was included in our prospective study, and he signed an informed consent form for further imaging. c) to e) ^{99m}Tc-MDP three-phase bone scan showed positive perfusion, blood pool, and delayed phase in the right knee (arrowheads) (red circle and region of interest of the affected side (ROIA); yellow circle and region of interest of the normal side (ROIB)). f) and g) SPECT/CT revealed focal increased bone metabolism at the right patella-prosthesis interface (arrowheads), and e) and f) the uniform and symmetrical uptake distributed along the edge of tibial and femoral component was regarded as non-specific uptake (dotted arrows). In addition, e) and g) show that focal uptake with hyperosteogeny was found on the medial articular surface of the left knee, which was considered to be OA (arrows). h) to l) ^{68}Ga-citrate PET/CT showed an obvious diffuse uptake around the right knee prosthesis (arrowheads). h), j), and l) PET/CT also showed a focal uptake in the left knee joint, which was consistent with the findings of SPECT/CT (arrows). Subsequently, the patient underwent surgical treatment. m) and n) Histopathological examination showed the presence of acute suppurative inflammation (m, haematoxylin and eosin (H&E) 100×; n, H&E 400×). *Staphylococcus epidermidis* was found in three of the five samples.

degree of inflammatory reaction associated with AL may be lower than that of PJI, and the inflammatory reaction of the former may be mainly limited to the articular surface that causes wear and tear. In addition, neutrophils are common in PJI, but the proportion of AL cases associated with non-specific inflammation is small (< 10%).[45,46] The difference in cell composition and inflammatory reaction between AL and PJI may explain the difference in ^{68}Ga-citrate uptake. However, the efficacy of semi-quantitative analysis parameter SUVmax in the differential diagnosis of AL and PJI was lower than that of all PET/CT visual analysis methods. Tseng et al[12] found that the SUVmax of ^{68}Ga-citrate PET/CT could not distinguish AL from PJI. In addition, some studies on ^{18}F-FDG[34,37,47,48] and ^{18}F-NaF[4,39] to differentiate PJI from AL have shown that the visual interpretation of site and pattern of uptake appeared more important and reliable than intensity of SUV. Therefore, focus on different uptake patterns of the tracer rather than through SUVmax in distinguishing AL from PJI may be a more accurate method.

The ^{68}Ga-citrate PET/CT uptake model had been proven to have a certain false negative rate (2/23) (Figure 4), which may limit its application in PJI. Two false negative patients in this study showed no tracer uptake. The result of bacterial culture in one patient was Gram-negative bacteria *Enterococcus faecalis*, but the bacterial culture of another patient failed and the diagnosis was confirmed by pathology and intraoperative findings. We suspect that false negative results may be associated with chronic low-grade bacterial infections, but our study cannot confirm this, as not all PJI patients have successfully cultured bacteria. In addition, AC may cause increased tracer uptake artifacts around the prosthesis of patients with metal implants.[49] However, the visual analysis of AC did not affect the results in this study whether at ten minutes or 60 minutes, and the diagnosis of AC is consistent with that of non-AC. In addition, the diagnostic efficiency of visual analysis at 60 minutes was higher than that at ten minutes. Therefore, imaging within 60 minutes may be a better choice.

Our study showed that three-phase bone scan had a very high sensitivity (100%) for the diagnosis of PJI, which was consistent with the results of Magnuson et al.[50] Therefore, PJI could be excluded when the three-phase bone scan was negative.[51,52] However, its specificity was limited and there was a high false positive rate in AL patients (6/16) (Figure 5).

In this study, we regarded focal periprosthetic uptake on SPECT/CT as AL, whereas diffuse uptake was associated with infection.[17,53] This visual analysis method had a high specificity (100%), but there was also a high false negative rate (4/23) (Figure 3), which was consistent

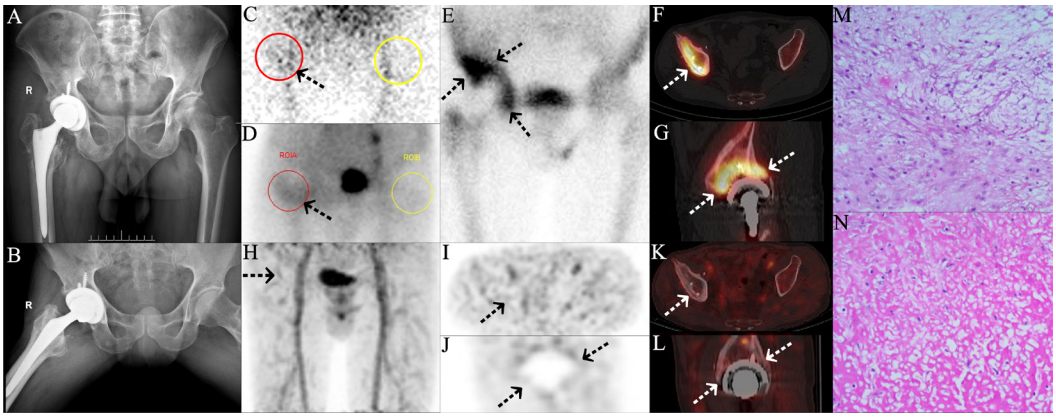

Fig. 4

True positive findings in the three-phase bone scan and single photon emission CT (SPECT)/CT, and false negative findings in positron emission tomography (PET)/CT, for infection in a patient with periprosthetic joint infection (PJI) confirmed by microbiological culture of *Enterobacter faecalis*. A 59-year-old man underwent a right hip arthroplasty for traumatic arthritis of the right hip after fracture of the right femur in 2012. Further, he underwent revision surgery for aseptic loosening (AL) of the right hip joint in 2019. He developed pain and swelling of the right hip joint one month ago. a) and b) No obvious positive signs were found in the anteroposterior (AP) and lateral radiographs postoperative at one year of the right hip joint. c) to e) ^{99m}Tc-MDP three-phase bone scan showed positive perfusion, blood pool, and delayed phase in right hip (arrows) (red circle and region of interest of the affected side (ROIA); yellow circle and region of interest of the normal side (ROIB)). f) and g) SPECT/CT revealed diffusely increased bone metabolism at the right acetabulum-prosthesis interface (arrows). h) to l) ^{68}Ga-citrate PET/CT showed no abnormal focal or diffuse uptake (arrows). Subsequently, the patient underwent surgical treatment. m) and n) Histopathological examination of synovial tissue showed chronic inflammatory changes (haematoxylin and eosin (H&E) 400×). However, *Enterobacter faecalis* was found in two of the five samples. PJI of the right hip was diagnosed.

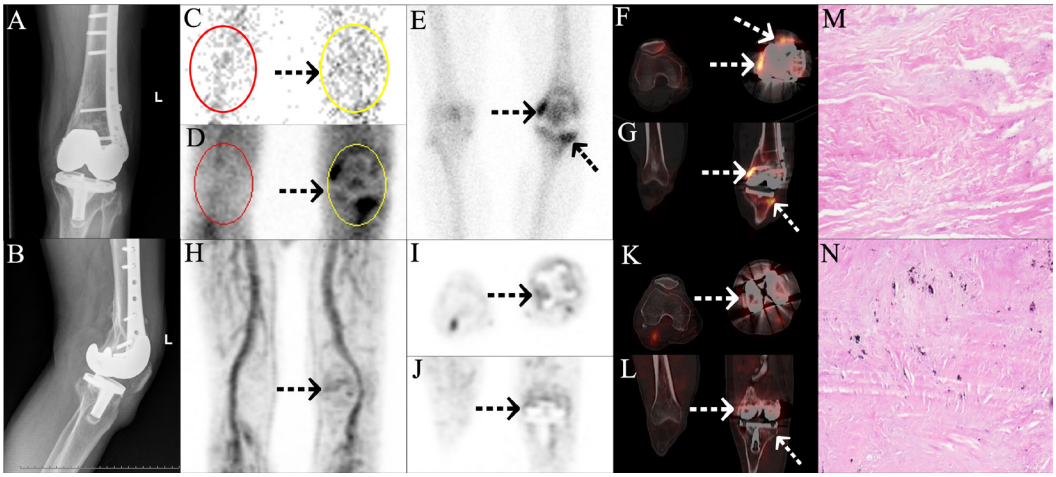

Fig. 5

False positive findings in three-phase bone scan and true negative findings in single-photon emission CT (SPECT)/CT and positron emission tomography (PET)/CT in a patient with aseptic loosening (AL). A 66-year-old man underwent left knee arthroplasty for traumatic osteoarthritis of the left knee after fracture of the left femur in 2009, and he developed pain in the left knee joint one week ago. a) and b) No obvious positive signs were found in the anteroposterior (AP) and lateral radiographs postoperative at ten years of the left knee joint. c) to e) ^{99m}Tc-MDP three-phase bone scan showed positive perfusion, blood pool, and delayed phase in the left knee (arrows) (red circles of c) to d) – region of interest of the affected side; yellow circles of c) to d) – region of interest of the normal side). f) and g) SPECT/CT revealed several points of focally increased bone metabolism at the bone-prosthesis interface of the left knee (arrows). h) to l) ^{68}Ga-citrate PET/CT showed mild uptake distributed uniformly and symmetrically along the edge of the prosthesis (arrows). The patient then underwent surgical treatment, and a large amount of proliferated synovial tissue was found; the prosthetic joint was obviously loose. m) and n) Histopathological examination showed proliferative fibrous connective tissue (haematoxylin and eosin (H&E) 400×). The postoperative microbial cultures were both negative. The patient was diagnosed with AL.

with the findings of Mountford et al.[54] The false negative on SPECT/CT may be related to the fact that some of the infected lesions occurred in the soft-tissue around the prosthesis rather than the bone-prosthesis interface. Compared to SPECT/CT, we found that ^{68}Ga-citrate may be concentrated around the soft-tissue with severe inflammatory reaction in PJI, while the tracer uptake at the bone-prosthesis interface may be relatively unclear (Figure 2). Therefore, the combination of the two imaging methods may have complementary value, especially for patients whose PJI mainly occurs in the soft-tissue around the prosthesis. Our combined models further confirmed

that the combination of SPECT/CT and AC at 60 minutes can improve the sensitivity.

There were some limitations to our study. First, the major limitation was its single-centre nature and the limited sample size. This might have affected the accuracy of our findings and prevented a more detailed analysis. A study with a larger sample size and more detailed assessment of the utility of ^{68}Ga-citrate is warranted. Second, our image analysis standards (including visual analysis and semi-quantitative analysis) of ^{68}Ga-citrate were formulated comprehensively based on experience from relevant studies of ^{18}F-NaF and ^{18}F-FDG, combined with the small number of existing studies of ^{68}Ga-citrate. Different evaluation criteria may lead to different research results, which is a potential flaw. In addition, there may be non-specific uptake on ^{99m}Tc-MDP bone scan within one to two years after prosthesis replacement,[15] and we did not study the potential effect of postoperative time on the diagnostic performance of various study parameters. More patient data are needed to analyze these variables properly in the future.

References

1. **Mandegaran R**, **Agrawal K**, **Vijayanathan S**, **Gnanasegaran G**. The value of 99mTc-MDP bone SPECT/CT in evaluation of patients with painful knee prosthesis. *Nucl Med Commun.* 2018;39(5):397–404.
2. **Staats K**, **Kolbitsch P**, **Sigmund IK**, **Hobusch GM**, **Holinka J**, **Windhager R**. Outcome of total hip and total knee revision arthroplasty with minor infection criteria: a retrospective matched-pair analysis. *J Arthroplasty.* 2017;32(4):1266–1271.
3. **Yue B**, **Tang T**. The use of nuclear imaging for the diagnosis of periprosthetic infection after knee and hip arthroplasties. *Nucl Med Commun.* 2015;36(4):305–311.
4. **Kumar R**, **Kumar R**, **Kumar V**, **Malhotra R**. Comparative analysis of dual-phase 18F-fluoride PET/CT and three phase bone scintigraphy in the evaluation of septic (or painful) hip prostheses: A prospective study. *J Orthop Sci.* 2016;21(2):205–210.
5. **Yagi H**, **Kihara S**, **Mittwede PN**, **et al**. Development of a large animal rabbit model for chronic periprosthetic joint infection. *Bone Joint Res.* 2021;10(3):156–165.
6. **Rupp M**, **Walter N**, **Baertl S**, **Lang S**, **Lowenberg DW**, **Alt V**. Terminology of bone and joint infection. *Bone Joint Res.* 2021;10(11):742–743.
7. **Gollwitzer H**, **Dombrowski Y**, **Prodinger PM**, **et al**. Antimicrobial peptides and proinflammatory cytokines in periprosthetic joint infection. *J Bone Joint Surg Am.* 2013;95-A(7):644–651.
8. **Zhuang H**, **Alavi A**. 18-fluorodeoxyglucose positron emission tomographic imaging in the detection and monitoring of infection and inflammation. *Semin Nucl Med.* 2002;32(1):47–59.
9. **Verberne SJ**, **Raijmakers PG**, **Temmerman OPP**. The accuracy of imaging techniques in the assessment of periprosthetic hip infection: a systematic review and meta-analysis. *J Bone Joint Surg Am.* 2016;98-A(19):1638–1645.
10. **Alt V**, **Rupp M**, **Langer M**, **Baumann F**, **Trampuz A**. Can the oncology classification system be used for prosthetic joint infection? The PJI-TNM system. *Bone Joint Res.* 2020;9(2):79–81.
11. **Wang Z**, **Cai L**, **Xu T**, **et al**. Comparative evaluation of 68ga-citrate PET/CT and 18F-FDG PET/CT in the diagnosis of type II collagen-induced arthritis in rats. *Contrast Media Mol Imaging.* 2019;2019:2353658.
12. **Tseng JR**, **Chang YH**, **Yang LY**, **et al**. Potential usefulness of 68Ga-citrate PET/CT in detecting infected lower limb prostheses. *EJNMMI Res.* 2019;9(1):2.
13. **SalomäkiSP**, **Kemppainen J**, **Hohenthal U**, **et al**. Head-to-head comparison of 68ga-citrate and 18F-FDG PET/CT for detection of infectious foci in patients with staphylococcus aureus bacteraemia. *Contrast Media Mol Imaging.* 2017;2017:3179607.
14. **World Medical Association**. World Medical Association Declaration of Helsinki: ethical principles for medical research involving human subjects. *JAMA.* 2013;310(20):2191–2194.
15. **Tam HH**, **Bhaludin B**, **Rahman F**, **Weller A**, **Ejindu V**, **Parthipun A**. SPECT-CT in total hip arthroplasty. *Clin Radiol.* 2014;69(1):82–95.
16. **Guan H**, **Xu C**, **Fu J**, **et al**. Diagnostic criteria of periprosthetic joint infection: a prospective study protocol to validate the feasibility of the 2018 new definition for Chinese patients. *BMC Musculoskelet Disord.* 2019;20(1):552.
17. **Vaz S**, **Ferreira TC**, **Salgado L**, **Paycha F**. Bone scan usefulness in patients with painful hip or knee prosthesis: 10 situations that can cause pain, other than loosening and infection. *Eur J Orthop Surg Traumatol.* 2017;27(2):147–156.
18. **Kobayashi N**, **Inaba Y**, **Choe H**, **et al**. Use of F-18 fluoride PET to differentiate septic from aseptic loosening in total hip arthroplasty patients. *Clin Nucl Med.* 2011;36(11):e156-61.
19. **Lee JW**, **Yu SN**, **Yoo ID**, **et al**. Clinical application of dual-phase F-18 sodium-fluoride bone PET/CT for diagnosing surgical site infection following orthopedic surgery. *Medicine (Baltimore).* 2019;98(11):e14770.
20. **Baertl S**, **Metsemakers WJ**, **Morgenstern M**, **et al**. Fracture-related infection. *Bone Joint Res.* 2021;10(6):351–353.
21. **Osmon DR**, **Berbari EF**, **Berendt AR**, **et al**. Diagnosis and management of prosthetic joint infection: clinical practice guidelines by the Infectious Diseases Society of America. *Clin Infect Dis.* 2013;56(1):e1–e25.
22. **Fang X**, **Zhang L**, **Cai Y**, **et al**. Effects of different tissue specimen pretreatment methods on microbial culture results in the diagnosis of periprosthetic joint infection. *Bone Joint Res.* 2021;10(2):96–104.
23. **Huang Z**, **Li W**, **Lee GC**, **et al**. Metagenomic next-generation sequencing of synovial fluid demonstrates high accuracy in prosthetic joint infection diagnostics: mNGS for diagnosing PJI. *Bone Joint Res.* 2020;9(7):440–449.
24. **Qin L**, **Li X**, **Wang J**, **Gong X**, **Hu N**, **Huang W**. Improved diagnosis of chronic hip and knee prosthetic joint infection using combined serum and synovial IL-6 tests. *Bone Joint Res.* 2020;9(9):587–592.
25. **Chen X**, **Li H**, **Zhu S**, **Wang Y**, **Qian W**. Is D-dimer a reliable biomarker compared to ESR and CRP in the diagnosis of periprosthetic joint infection? a systematic review and meta-analysis. *Bone Joint Res.* 2020;9(10):701–708.
26. **Trotter AJ**, **Dean R**, **Whitehouse CE**, **et al**. Preliminary evaluation of a rapid lateral flow calprotectin test for the diagnosis of prosthetic joint infection. *Bone Joint Res.* 2020;9(5):202–210.
27. **Yang B**, **Fang X**, **Cai Y**, **et al**. Detecting the presence of bacterial RNA by polymerase chain reaction in low volumes of preoperatively aspirated synovial fluid from prosthetic joint infections. *Bone Joint Res.* 2020;9(5):219–224.
28. **Li R**, **Wang C**, **Ji XJ**, **et al**. Centrifugation may eliminate false-positive leucocyte esterase strip test results caused by inflammatory arthritis in the diagnosis of knee infection: A pilot study. *Bone Joint Res.* 2020;9(5):236–241.
29. **Zhang Z**, **Cai Y**, **Bai G**, **et al**. The value of calprotectin in synovial fluid for the diagnosis of chronic prosthetic joint infection. *Bone Joint Res.* 2020;9(8):450–457.
30. **Akhbari P**, **Jaggard MK**, **Boulangé CL**, **et al**. Differences between infected and noninfected synovial fluid. *Bone Joint Res.* 2021;10(1):85–95.
31. **Qin L**, **Hu N**, **Li X**, **Chen Y**, **Wang J**, **Huang W**. Evaluation of synovial fluid neutrophil CD64 index as a screening biomarker of prosthetic joint infection. *Bone Joint J.* 2020;102-B(4):463–469.
32. **Kim K**, **Kim SJ**. Diagnostic role of PET or PET/CT for prosthetic joint infection: A systematic review and Meta-analysis. *Hell J Nucl Med.* 2021;24(1):83–93.
33. **Aksoy SY**, **Asa S**, **Ozhan M**, **et al**. FDG and FDG-labelled leucocyte PET/CT in the imaging of prosthetic joint infection. *Eur J Nucl Med Mol Imaging.* 2014;41(3):556–564.
34. **Verberne SJ**, **Temmerman OPP**, **Vuong BH**, **Raijmakers PG**. Fluorodeoxyglucose positron emission tomography imaging for diagnosing periprosthetic hip infection: the importance of diagnostic criteria. *Int Orthop.* 2018;42(9):2025–2034.
35. **Stumpe KDM**, **Nötzli HP**, **Zanetti M**, **et al**. FDG PET for differentiation of infection and aseptic loosening in total hip replacements: comparison with conventional radiography and three-phase bone scintigraphy. *Radiology.* 2004;231(2):333–341.
36. **Kiran M**, **Donnelly TD**, **Armstrong C**, **Kapoor B**, **Kumar G**, **Peter V**. Diagnostic utility of fluorodeoxyglucose positron emission tomography in prosthetic joint infection based on MSIS criteria. *Bone Joint J.* 2019;101-B(8):910–914.
37. **Reinartz P**, **Mumme T**, **Hermanns B**, **et al**. Radionuclide imaging of the painful hip arthroplasty: positron-emission tomography versus triple-phase bone scanning. *J Bone Joint Surg Br.* 2005;87-B(4):465–470.
38. **Falstie-Jensen T**, **Lange J**, **Daugaard H**, **et al**. 18F FDG-PET/CT has poor diagnostic accuracy in diagnosing shoulder PJI. *Eur J Nucl Med Mol Imaging.* 2019;46(10):2013–2022.
39. **Koob S**, **Gaertner FC**, **Jansen TR**, **et al**. Diagnosis of peri-prosthetic loosening of total hip and knee arthroplasty using 18F-Fluoride PET/CT. *Oncotarget.* 2019;10(22):2203–2211.
40. **Lankinen P**, **Noponen T**, **Autio A**, **et al**. A comparative 68ga-citrate and 68ga-chloride PET/CT imaging of Staphylococcus aureus osteomyelitis in the rat tibia. *Contrast Media Mol Imaging.* 2018;2018:9892604.

41. **El-Maghraby TA**, **Moustafa HM**, **Pauwels EK**. Nuclear medicine methods for evaluation of skeletal infection among other diagnostic modalities. *Q J Nucl Mol Imaging*. 2006;50(3):167–192.
42. **Mushtaq N**, **To K**, **Gooding C**, **Khan W**. Radiological imaging evaluation of the failing total hip replacement. *Front Surg*. 2019;6:35.
43. **Abu-Amer Y**, **Darwech I**, **Clohisy JC**. Aseptic loosening of total joint replacements: mechanisms underlying osteolysis and potential therapies. *Arthritis Res Ther*. 2007;9 Suppl 1:S6.
44. **Palestro CJ**. Nuclear medicine and the failed joint replacement: Past, present, and future. *World J Radiol*. 2014;6(7):446–458.
45. **Love C**, **Tomas MB**, **Marwin SE**, **Pugliese PV**, **Palestro CJ**. Role of nuclear medicine in diagnosis of the infected joint replacement. *Radiographics*. 2001;21(5):1229–1238.
46. **Sigmund IK**, **McNally MA**, **Luger M**, **Böhler C**, **Windhager R**, **Sulzbacher I**. Diagnostic accuracy of neutrophil counts in histopathological tissue analysis in periprosthetic joint infection using the ICM, IDSA, and EBJIS criteria. *Bone Joint Res*. 2021;10(8):536–547.
47. **Chacko TK**, **Zhuang H**, **Nakhoda KZ**, **Moussavian B**, **Alavi A**. Applications of fluorodeoxyglucose positron emission tomography in the diagnosis of infection. *Nucl Med Commun*. 2003;24(6):615–624.
48. **Kwee RM**, **Kwee TC**. 18F-FDG PET for diagnosing infections in prosthetic joints. *PET Clin*. 2020;15(2):197–205.
49. **Goerres GW**, **Ziegler SI**, **Burger C**, **Berthold T**, **Von Schulthess GK**, **Buck A**. Artifacts at PET and PET/CT caused by metallic hip prosthetic material. *Radiology*. 2003;226(2):577–584.
50. **Magnuson JE**, **Brown ML**, **Hauser MF**, **Berquist TH**, **Fitzgerald RH**, **Klee GG**. In-111-labeled leukocyte scintigraphy in suspected orthopedic prosthesis infection: comparison with other imaging modalities. *Radiology*. 1988;168(1):235–239.
51. **Kim C**, **Lee SJ**, **Kim JY**, **Hwang KT**, **Choi YY**. Comparative analysis of 99mTc-MDP three-phase bone scan with SPECT/CT and 99mTc-HMPAO-labeled WBC SPECT/CT in the differential diagnosis of clinically suspicious post-traumatic osteomyelitis. *Nucl Med Mol Imaging*. 2017;51(1):40–48.
52. **Romanò CL**, **Petrosillo N**, **Argento G**, **et al**. The role of imaging techniques to define a peri-prosthetic hip and knee joint infection: multidisciplinary consensus statements. *J Clin Med*. 2020;9(8):E2548.
53. **Williamson BR**, **McLaughlin RE**, **Wang GW**, **Miller CW**, **Teates CD**, **Bray ST**. Radionuclide bone imaging as a means of differentiating loosening and infection in patients with a painful total hip prosthesis. *Radiology*. 1979;133(3 Pt 1):723–725.
54. **Mountford PJ**, **Hall FM**, **Wells CP**, **Coakley AJ**. 99Tcm-MDP, 67Ga-citrate and 111In-leucocytes for detecting prosthetic hip infection. *Nucl Med Commun*. 1986;7(2):113–120.

Author information:
- T. Xu, MD, Physician
- X. Yang, MD, Physician
- G. Liu, MBBS, Technician
- T. Lv, PhD, Research Fellow
- F. Jiang, MD, PhD, Research Fellow
- Y. Chen, MD, Physician

Department of Nuclear Medicine, The Affiliated Hospital of Southwest Medical University, Luzhou, China; Nuclear Medicine and Molecular Imaging Key Laboratory of Sichuan Province, Luzhou, China; Institute of Nuclear Medicine, Southwest Medical University, Luzhou, Sichuan, China.

- Y. Zeng, MD, Surgeon
- H. Yang, MD, Surgeon

Department of Orthopedics, The Affiliated Hospital of Southwest Medical University, Luzhou, China.

Author contributions:
- T. Xu: Conceptualization, Data curation, Formal analysis, Investigation, Visualization, Writing – original draft, Writing – review & editing.
- Y. Zeng: Conceptualization, Data curation, Formal analysis, Investigation, Visualization.
- X. Yang: Conceptualization, Data curation, Formal analysis, Visualization.
- G. Liu: Methodology, Software.
- T. Lv: Methodology, Resources.
- H. Yang: Methodology, Resources, Validation, Visualization.
- F. Jiang: Methodology, Resources, Supervision, Validation, Visualization.
- Y. Chen: Methodology, Resources, Supervision, Project administration, Validation, Visualization, Writing – review & editing.

- T. Xu, Y. Zeng, and X. Yang contributed equally to this work.
- H. Yang, F. Jiang, and Y. Chen contributed equally to this work.
- T. Xu, Y. Zeng, and X. Yang are joint first authors.
- H. Yang, F. Jiang, and Y. Chen are joint senior authors.

Funding statement:
- The authors disclose receipt of the following financial or material support for the research, authorship, and/or publication of this article: financial support from the National Natural Science Foundation of China (Project U20A20384).

ICMJE COI statement:
- The authors declare that they have no competing interests.

Acknowledgements:
- We are grateful to H. Ding for helping us with image analysis. We would like to thank Editage (www.editage.com) for English language editing. We are grateful to the members of Department of Nuclear Medicine, The Affiliated Hospital, Southwest Medical University and Nuclear Medicine and Molecular Imaging Key Laboratory of Sichuan Province for their technical guidance, cooperation, and assistance in completing this study.

Ethical review statement:
- All procedures were carried out in accordance with the principles of the Helsinki Declaration. This study was approved by the ethics committee of the Affiliated Hospital of Southwest Medical University. All patients signed an informed consent form approved by the Institutional Review Board after the nature and significance of the imaging study had been fully explained to them.

Open access funding
- The authors report that the open access funding for their manuscript was self-funded.